Overexpression of PLIN5 in skeletal muscle promotes oxidative gene expression and intramyocellular lipid content without compromising insulin sensitivity.

Biochimica et Biophysica Acta 1831 (2013) 844–852

Contents lists available at SciVerse ScienceDirect

Biochimica et Biophysica Acta

journal homepage: www.elsevier.com/locate/bbalip

Overexpression of PLIN5 in skeletal muscle promotes oxidative gene expression and intramyocellular lipid content without compromising insulin sensitivity

M. Bosma [a], L.M. Sparks [a], G.J. Hooiveld [b], J.A. Jorgensen [a], S.M. Houten [c], P. Schrauwen [a], S. Kersten [b], M.K.C. Hesselink [d,*]

[a] Department of Human Biology, NUTRIM, Maastricht University Medical Centre +, Maastricht, The Netherlands
[b] Nutrition, Metabolism and Genomics group, Division of Human Nutrition, Wageningen University, Wageningen, The Netherlands
[c] Laboratory Genetic Metabolic Diseases, Departments of Clinical Chemistry and Pediatrics, Emma Children's Hospital, Academic Medical Center, University of Amsterdam, Amsterdam, The Netherlands
[d] Department of Human Movement Sciences, NUTRIM, Maastricht University Medical Centre +, Maastricht, The Netherlands

ARTICLE INFO

Article history:
Received 16 August 2012
Received in revised form 6 January 2013
Accepted 10 January 2013
Available online 22 January 2013

Keywords:
Lipid droplet
Perilipin
OXPAT
Skeletal muscle
Insulin sensitivity
Oxidative gene expression

ABSTRACT

Aims/hypothesis: While lipid deposition in the skeletal muscle is considered to be involved in obesity-associated insulin resistance, neutral intramyocellular lipid (IMCL) accumulation *per se* does not necessarily induce insulin resistance. We previously demonstrated that overexpression of the lipid droplet coat protein perilipin 2 augments intramyocellular lipid content while improving insulin sensitivity. Another member of the perilipin family, perilipin 5 (PLIN5), is predominantly expressed in oxidative tissues like the skeletal muscle. Here we investigated the effects of PLIN5 overexpression – in comparison with the effects of PLIN2 – on skeletal muscle lipid levels, gene expression profiles and insulin sensitivity. *Methods*: Gene electroporation was used to overexpress PLIN5 in tibialis anterior muscle of rats fed a high fat diet. Eight days after electroporation, insulin-mediated glucose uptake in the skeletal muscle was measured by means of a hyperinsulinemic euglycemic clamp. Electron microscopy, fluorescence microscopy and lipid extractions were performed to investigate IMCL accumulation. Gene expression profiles were obtained using microarrays. *Results*: TAG storage and lipid droplet size increased upon PLIN5 overexpression. Despite the higher IMCL content, insulin sensitivity was not impaired and DAG and acylcarnitine levels were unaffected. In contrast to the effects of PLIN2 overexpression, microarray data analysis revealed a gene expression profile favoring FA oxidation and improved mitochondrial function. *Conclusions/interpretation*: Both PLIN2 and PLIN5 increase neutral IMCL content without impeding insulin-mediated glucose uptake. As opposed to the effects of PLIN2 overexpression, overexpression of PLIN5 in the skeletal muscle promoted expression of a cluster of genes under control of PPARα and PGC1α involved in FA catabolism and mitochondrial oxidation.

1. Introduction

Obesity is associated with increased lipid supply to the skeletal muscle resulting in increased intramyocellular lipid (IMCL) storage. Accumulation of IMCL is associated with the development of insulin resistance. However, IMCL accumulation *per se* does not necessarily induce insulin resistance (reviewed in [1]). Recent studies suggest that increasing the capacity for triacylglycerol (TAG) storage in lipid droplets (LDs) creates a sink for storage of fatty acids (FAs) in the form of neutral lipids thereby sequestering FAs and protecting against lipotoxicity [2–5].

By regulating processes like LD synthesis, breakdown, fusion, intracellular transport and interorganelle interactions, LD coat proteins are determinants of the highly dynamic nature of LDs (reviewed in [6,7]). One of the major lipid droplet coat protein families characterized to date is the perilipin family. Perilipin 2 (PLIN2), PLIN3 and PLIN5 are considered the major perilipins in the skeletal muscle. Indeed, we have recently shown that PLIN2 overexpression in the muscle results in massive fat accumulation in the muscle, while insulin-mediated glucose uptake was only modestly increased [2]. Furthermore, PLIN2 overexpression also blunted high fat diet-induced induction of expression of OXPHOS protein complexes [2], which may indicate that in the long run oxidative capacity will no longer keep track with intramyocellular lipid content in this situation.

Abbreviations: ATGL, adipose triglyceride lipase; CGI-58, comparative gene identification-58; DAG, diacylglycerol; FA, fatty acid; GO, gene ontology; GSEA, gene set enrichment analysis; IMCL, intramyocellular lipid; LD, lipid droplet; NES, normalized enrichment score; PLIN, perilipin; TA, tibialis anterior; TAG, triacylglycerol

* Corresponding author at: Department of Human Movement Sciences, NUTRIM School for Nutrition, Toxicology and Metabolism, Maastricht University Medical Centre +, 6200MD Maastricht, The Netherlands. Tel.: +31 43 3881317; fax: +31 43 3670972.
E-mail address: matthijs.hesselink@maastrichtuniversity.nl (M.K.C. Hesselink).

1388-1981/$ – see front matter © 2013 Elsevier B.V. All rights reserved.
http://dx.doi.org/10.1016/j.bbalip.2013.01.007

Why the skeletal muscle expresses both PLIN2 and PLIN5 is still unknown. We and others [8,9] recently found that PLIN5 not only localizes to LDs, but also to the mitochondria. Thus, the putative role of PLIN5 is most likely not limited to the regulation of lipolysis. Putatively, PLIN5 may also be involved in shuttling of FAs to the mitochondria for oxidation. In line with this we observed that PLIN5 overexpression also augmented intramyocellular LD content in parallel with improved oxidation of palmitate to CO_2 [8]. Here, we aimed to further investigate the effects of PLIN5 overexpression – in comparison with effects of PLIN2 – on lipid storage, transcriptomic oxidative gene profiles, and insulin sensitivity.

2. Materials and methods

2.1. Study design

8-week old male Wistar rats were purchased from Charles River (Wilmington, Massachusetts, USA). Rats were housed individually on a 12:12 h light–dark cycle (light from 7:00 am to 7:00 pm), at room temperature (21–22 °C) with *ad libitum* access to tap water. Rats were fed a high fat diet (45% energy from fat, D01060502, Research Diets, New Brunswick, NJ, USA) for the duration of the 3-week intervention. The study complied with the 'Principles of laboratory animal care' (NIH publication no. 85-23, revised 1985; http://grants1.nih.gov/grants/olaw/references/phspol.htm) and The Animal Care and Use Committee of Maastricht University approved the experiments (approval number 2010-036). During the experiments all efforts were made to minimize suffering of the animals.

2.2. Electroporation

Two weeks after the start of the diet, overexpression of *Plin5* in either the right or left tibialis anterior (TA) muscle of the rat was accomplished by an *in vivo* DNA electrotransfer technique to achieve overexpression of PLIN5 in one leg; the contralateral TA served as a sham-electroporated internal control. *Plin5* was electroporated randomly in the left or the right TA. DNA electroporation was performed under isoflurane anesthesia. TA muscles were transcutaneously injected with either 150 μg (2 μg/μl) pcDNA3.1-CMV-*Plin5* or pcDNA3.1-empty vector in 0.9% sterile saline. Within 15 s after the last injection 5 electric pulses were applied by two stainless steel plate electrodes placed at the ventral and dorsal side of the leg. One high voltage pulse of 800 V/cm and four low voltage pulses of 80 V/cm at 1 Hz were generated by an ECM 830 electroporator (BTX, San Diego, CA, USA) as described previously [10,11]. Rats were killed 8 days post-electroporation. TA muscles were quickly dissected and processed for mitochondrial isolations and morphological analysis. The remainder of the TA was rapidly frozen in melting isopentane for further analyses.

2.3. Cannulation and hyperinsulinemic euglycemic clamps

Throughout the entire study, rats were handled daily for familiarization. Indwelling catheters were placed in the right jugular vein (for the sampling of blood) and the left carotid artery (for the infusion of insulin and glucose) under isoflurane anesthesia and aseptic conditions, two weeks before the hyperinsulinemic euglycemic clamp was performed. The venous catheter was extended to the level of the right atrium and the arterial catheter within the aortic arch. Both catheters were tunnelled subcutaneously and exteriorized at the top of the head, where they were attached in dentist cement between 2 and 3 screws onto a 90°-bend needle. The catheters were filled with a mixture of 85% glycerol (Merck, Darmstadt, Germany) and 500 U/ml heparin (Leo Pharma BV, Breda, The Netherlands) to maintain patency. All rats regained pre-surgery body mass within 3 days.

Hyperinsulinemic euglycemic clamps of conscious rats were performed after a 6 h fast. Insulin stimulated glucose disposal *in vivo* within the individual tibialis anterior muscles was studied according to a previously described method [12]. A primed continuous infusion of insulin (Actrapid HM; Novo Nordisk, Copenhagen, Denmark) was administered at a rate of 13 mU/kg/min for 120 min. Blood glucose values were monitored at 10-min intervals throughout the clamp. The glucose infusion rate (GIR) was adjusted to maintain blood glucose concentration within the range of 3.5–4.5 mM. Rats were conscious during the entire clamp. 45 min before completion of the clamp, a bolus of 140 μCi/kg of the non-metabolizable glucose analogue 2-[^{3}H(N)]-deoxy-D-glucose (Perkin Elmer, Waltham, Massachusetts, USA) was administered to measure insulin-stimulated glucose disposal in the individual TA muscles. Upon completion of the clamp, the rats were sacrificed with an overdose of sodium pentobarbital and tibialis anterior muscles were quickly dissected and frozen in liquid nitrogen-cooled isopentane and stored at −80 °C until further analyses.

2.4. ^{3}H-deoxyglucose measurements

Frozen TA muscle sections were ground to powder under liquid nitrogen, homogenized in MilliQ water, and eluted on columns filled with DOWEX ion-exchange resin (Sigma, St. Louis, Missouri, USA) using elution buffer (0.3 M ammonium acetate and 1.25% formic acid in H_2O, pH 4.9). Ionizing radiation counts were determined by scintillation counting.

2.5. ^{14}C-palmitate oxidation assays

Palmitate oxidation was determined in skeletal muscle homogenates as previously described [13]. Briefly, muscle was homogenized in a buffer (pH 7.4) containing 250 mM sucrose, 10 mM Tris–HCl, 2 mM ATP and 1 mM EDTA (Sigma, St. Louis, USA). This method does not affect mitochondrial morphology and function [14]. Subsequently, the muscle homogenates were plated in triplicate into a modified 48-well trapping device [15]. A small groove was engineered between adjacent wells so that CO_2 could freely diffuse between the incubation and trap wells. Reactions were started with the addition of reaction media yielding final concentrations (in mM) of 0.2 palmitate and 0.0175 [1-^{14}C]-palmitate and 125 sucrose, 20 Tris–HCl, 25 KH_2PO_4, 200 KCL, 2.5 MgCl, 0.25 malate, 4 ATP, 2.5 DTT, 2.5 carnitine, 0.125 coenzyme A, and 0.25 NAD^+. Palmitate was coupled to FA-free BSA in a molar ratio of 5:1. Trapping devices were sealed with a siliconized rubber gasket and incubated at 37 °C. After 2 h, reactions were terminated in the sealed reaction plates by the addition of 70% perchloric acid to the incubation wells. Perchloric acid also results in precipitation of the remaining FAs in the media. The trapping device was transferred to an orbital shaker, and $^{14}CO_2$ was trapped in the adjoining well in 1 N NaOH for 1 h. The acidified medium was stored at 4 °C overnight, and then acid soluble metabolites (ASMs) were assayed in supernatants of the acid precipitate. Radioactivity of CO_2 and ASMs was determined by liquid scintillation counting by use of 5 ml of Hionic Fluor (Perkin Elmer, Boston, USA). Data were normalized to protein content.

2.6. Electron microscopy procedures

Ultrastructural morphology was examined using transmission electron microscopy. Muscle tissue sections were fixed in 2.5% glutaraldehyde in 0.1 M phosphate buffer (pH 7.4). Postfixation was performed in 1% osmium tetroxide in 0.1 M cacodylate buffer (pH 7.4) supplemented with 1.5% potassium ferrocyanide. The samples were then dehydrated and embedded in epon. Ultrathin sections were examined using a Philips CM100 electron microscope. Electron microscopy pictures were available from 4 rats. 5–10 images per muscle sample were taken randomly. LD size was measured using the freehand selection tool of ImageJ [16].

2.7. Oil-red-O staining and immunofluorescence

Neutral lipids were stained in the muscle sections with a modified Oil-red-O staining along with immunofluorescence to study PLIN5 and laminin using antibodies against PLIN5 (#GP31; Progen Biotechnik, Heidelberg, Germany) and laminin (L-9393; Sigma, St. Louis, USA) as previously described [17] and visualized with appropriate secondary Alexafluor conjugated antibodies (Invitrogen, Groningen, The Netherlands).

2.8. Lipid profiles

Intramyocellular TAG levels were measured using the method of Schwartz and Wolins [18]. DAG [2] and acylcarnitine [19] levels were measured as described previously.

2.9. Western blots

Western blots were performed with muscle homogenates in RIPA-lysis buffer mixed 1:1 with Laemmli sample buffer (Bio-Rad, Mississauga, Ontario, Canada) using antibodies directed against PLIN2 (GP40; Progen, Heidelberg, Germany), PLIN3 (SC-14726, Santa Cruz Biotechnology, Heidelberg, Germany), PLIN5 (GP31; Progen, Heidelberg, Germany), ATGL (2138, Cell Signaling, Boston, USA), CGI-58 (NB110-41576, Novus Biologicals, Littleton, USA), and HSL (4107, Cell Signaling, Boston, USA). Secondary antibodies for PLIN2, PLIN3 PLIN5, ATGL and SR-actin contained a fluorescent tag (IRDye800- or IRDye700-conjugated secondary antibodies (Rockland, Tebu-bio, Heerhugowaard, The Netherlands, and LICOR Biosciences, Westburg, Leusden, The Netherlands). Protein quantification was performed by scanning on an Odyssey Infrared Imaging system (LI-COR Biotechnology, Lincoln, Nebraska, USA). CGI-58 and HSL were detected using an HRP-conjugated antibody and ECL detection. Protein expression values were standardized against sr-actin protein expression (Sigma, St. Louis, USA) and expressed in arbitrary units (AU).

2.10. RNA isolation and microarray gene expression analysis

Total RNA from rat tibialis anterior muscle was extracted and purified with the RNeasy kit for fibrous tissue (Qiagen, Venlo, The Netherlands). RNA quality was assessed on an Agilent 2100 bioanalyzer (Agilent Technologies, Amsterdam, The Netherlands) with 6000 Nano Chips using the Eukaryote Total RNA Nano assay. RNA was judged as suitable for array hybridization only if samples showed intact bands corresponding to the 28S and 18S rRNA subunits, displayed no chromosomal peaks or RNA degradation products, and had a RIN (RNA integrity number) above 8.0. RNA samples from 6 rats were pooled. Five micrograms of RNA were used for one cycle cRNA synthesis (Affymetrix, Santa Clara, CA). Hybridization, washing and scanning of Affymetrix rat arrays was carried out according to standard Affymetrix protocols. To adjust for non-specific hybridization and optical noise, the array expression data were normalized with RMA (robust multichip analysis, a package of the Bioconductor project [20] in the R environment. Functional analysis of the array data was performed by a method based on enrichment of gene sets (Gene Ontology (GO) classes using the application GSEA [21] and gene set clustering analysis using Cytoscape [22].

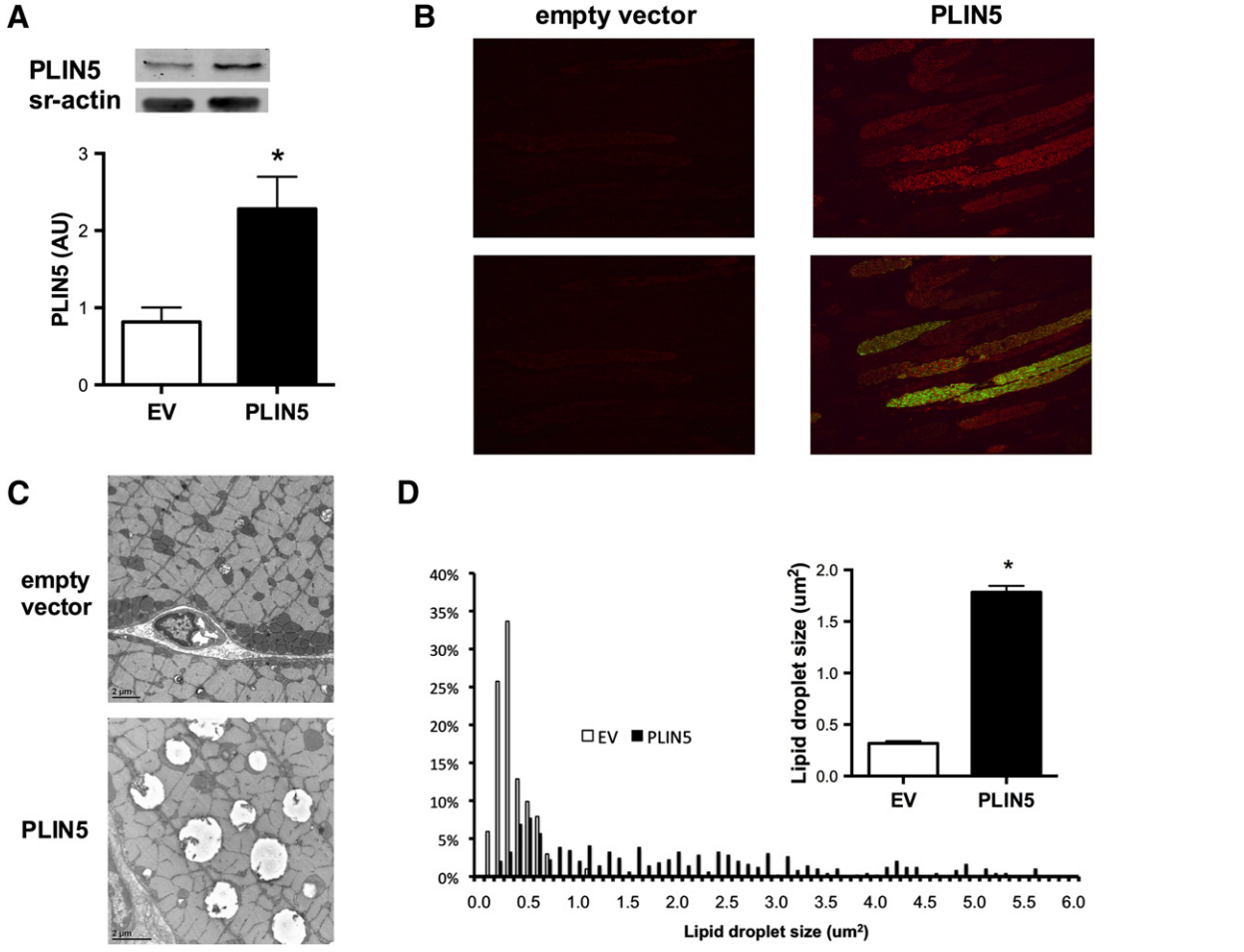

Fig. 1. PLIN5 overexpression increases intramyocellular lipid accumulation and lipid droplet size. (A) PLIN5 protein content in protein lysates from electroporated tibialis anterior muscle. (B) Shows the effect of PLIN5 overexpression on PLIN5 content (lower right hand panel) and lipid storage (upper right hand panel) compared to the empty vector control (upper and lower left hand panels). LDs are stained in red, PLIN5 in green and cell membranes in blue. Bars represent 100 μm. (C) Electron microscopy showing skeletal muscle ultrastructure. (D) Lipid droplet size distribution and average LD size. EV: empty vector, *P<0.05, error bars represent SEM.

Microarray data have been submitted to Gene Expression Omnibus (GEO number pending).

2.11. Statistical analysis

Results are presented as mean ± SEM. Differences between groups were evaluated with paired T-tests. Outcomes were considered statistically significant when $P<0.05$ (two-tailed). Analyses were performed using the Statistical Package for the Social Sciences (SPSS 16.0, Nieuwegein, The Netherlands) software for Mac 16.0. For microarray data, normalized enrichment scores (NES) and false discovery rates (q-values), calculated by the application GSEA, were reported. Q-values <0.05 were considered statistically significant. In Cytoscape, cut-off values were set at $P<0.005$ and $q<0.1$.

3. Results

3.1. PLIN5 overexpression increases intramyocellular lipid storage

PLIN5 electroporation resulted in a 2.8-fold overexpression of PLIN5 (empty vector muscle lysates 0.81 ± 0.19, PLIN5 muscle 2.28 ± 0.42 AU, $P<0.05$, $n=9$) (Fig. 1A). The overexpression of PLIN5 gave rise to a pronounced increase in IMCL levels (Fig. 1B–C). Lipid droplet size was increased; the LD size distribution shifted from LDs of up to 1.2 μm^2 in size in the empty vector-electroporated muscle fibers to LDs of up to 5.8 μm^2 in the PLIN5 overexpressing fibers (Fig. 1D). The average LD size increased more than five-fold ($P<0.01$) (Fig. 1D). The increase in LD size occurred in parallel with a 3-fold increase in intramyocellular triacylglycerol (TAG) levels (Fig. 2A). Diacylglycerol (DAG) levels (Fig. 2B) were unchanged. Acylcarnitines are formed in mitochondria when β-oxidation rates outpace the capacity of the TCA cycle [23] and have been implemented in development of insulin resistance. Free carnitine (Fig. 2C) and acylcarnitine levels (Fig. 2D) were not different in the PLIN5-electroporated muscle versus the empty vector control. Additionally, the FA-composition of the DAG fraction was not significantly changed and the individual acylcarnitine species did not show a different profile in empty-vector versus PLIN5-electroporated muscles (Supplemental Tables S1 and S2, respectively).

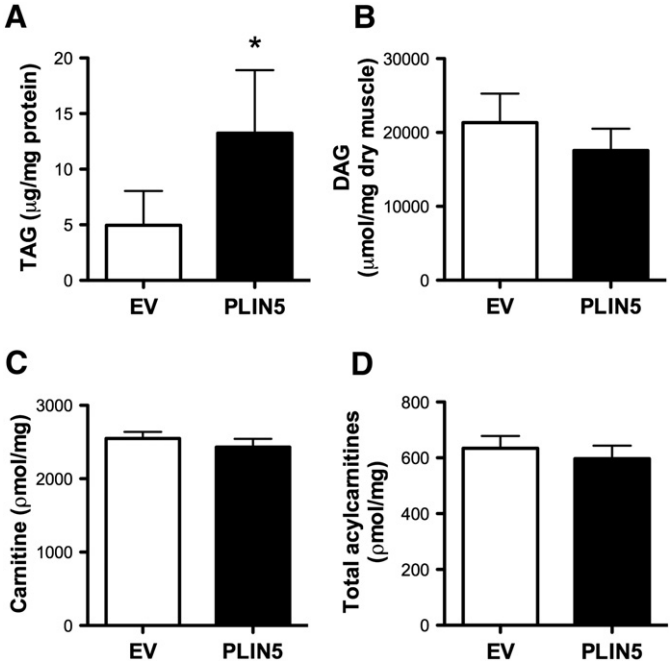

Fig. 2. PLIN5 overexpression results in increased TAG accumulation. (A) Skeletal muscle TAG levels (ug/mg protein). (B) DAG content (μmol/mg dry weight). (C) Free carnitine (ρmol/mg protein). (D) Acylcarnitine levels (ρmol/mg protein). EV: empty vector, *$P<0.05$, error bars represent SEM.

3.2. Increased ATGL protein content in PLIN5 overexpressing muscle

PLIN5 overexpression was not paralleled by compensatory changes in PLIN2 and PLIN3 protein content (Fig. 3A and B). ATGL protein content was significantly increased by 16% ($P=0.047$) (Fig. 3C), while CGI-58 protein content showed a trend towards downregulation ($P=0.10$) (Fig. 3D). HSL protein content was similar in empty vector and PLIN5-electroporated muscle (Fig. 3E).

3.3. PLIN5 overexpression results in a gene expression pattern favoring FA oxidative metabolism

Upon PLIN5 overexpression, 775 genes were upregulated, 1042 genes were downregulated (fold change cut-off value 1.3). Table 1 gives the gene expression profiles for a selection of genes, the complete microarray dataset can be found as supporting document online (Supplemental Table S3, GEO accession number: GSE43832). Gene class enrichment analyses revealed that PLIN5 overexpression resulted in increased expression of genes involved in FA β-oxidation, the TCA cycle, the electron transport chain and mitochondrion organization (Table 2). Genes involved in immune processes were downregulated (Table 3). To investigate if these gene expression profiles were specific

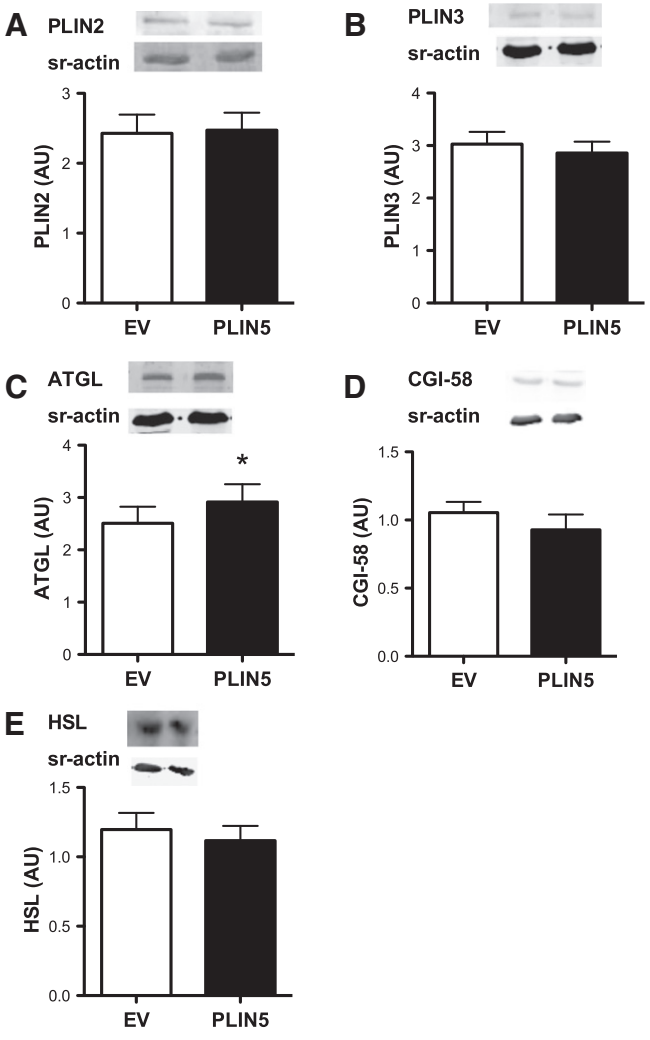

Fig. 3. PLIN5 overexpression increased ATGL protein content. (A–D) Western blots for PLIN2 (A), PLIN3 (B), ATGL (C), CGI-58 (D) and HSL (E) in whole muscle protein lysates ($n=17$).

Table 1
Heat map. Fold changes in gene expression for a selection of genes are given for PLIN5 versus empty-vector electroporated muscles.

Gene name	Entrez ID	Description	Fold change PLIN5 vs EV
Pla2g4c	691810	Phospholipase A2, group IVC (cytosolic, calcium-independent)	2.94
Acsm5	361637	Acyl-CoA synthetase medium-chain family member 5	2.17
Scand3	288622	SCAN domain containing 3	2.17
LOC679586	679586	Similar to ATP synthase, H+transporting, mitochondrial F0 complex, subunit G	1.89
Atp5hl1	306478	ATP synthase, H+transporting, mitochondrial F0 complex, subunit d-like 1	1.78
Dync2li1	298767	Dynein cytoplasmic 2 light intermediate chain 1	1.77
Acat3	308100	Acetyl-Coenzyme A acetyltransferase 3	1.70
Rfk	499328	Riboflavin kinase	1.70
Angptl4	362850	Angiopoietin-like 4	1.68
Atp6v1a	685232	ATPase, H+transporting, lysosomal V1 subunit A	1.63
Hsd3b	682974	3 beta-hydroxysteroid dehydrogenase/delta-5-delta-4 isomerase type II	1.59
Fabp4	79451	Fatty acid binding protein 4	1.58
Acot3	314304	Acyl-CoA thioesterase 3	1.57
Acnat1	681043	Acyl-coenzyme A amino acid N-acyltransferase 1	1.55
LOC689271	689271	Similar to ATP synthase, H+ transporting, mitochondrial F0 complex, subunit f, isoform 2	1.54
RGD1559672	500650	Similar to Translocase of inner mitochondrial membrane 23 homolog	1.48
Nkain3	689576	Na+/K+ transporting ATPase interacting 3	1.47
Ehhadh	171142	Enoyl-Coenzyme A, hydratase/3-hydroxyacyl Coenzyme A dehydrogenase	1.45
Atp6v1b1	312488	ATPase, H transporting, lysosomal V1 subunit B1	1.41
Atp6v1g3	289407	ATPase, H+ transporting, lysosomal V1 subunit G3	1.38
Fads6	303671	Fatty acid desaturase domain family, member 6	1.35
Mrps27	361883	Mitochondrial ribosomal protein S27	1.34
Acox2	252898	Acyl-Coenzyme A oxidase 2, branched chain	1.33
RGD1561341	502769	Similar to translocase of outer mitochondrial membrane 20 homolog	1.33
Pld6	287366	Phospholipase D family, member 6	1.33
Atp5s	362749	ATP synthase, H+transporting, mitochondrial F0 complex, subunit s (factor B)	1.32
Slc27a3	295219	Solute carrier family 27 (fatty acid transporter), member 3	−2.98
Pparg	25664	Peroxisome proliferator-activated receptor gamma	−1.89
Gk5	367146	Glycerol kinase 5 (putative)	−1.79
Ppt1	29411	Palmitoyl-protein thioesterase 1	−1.70
Sln	367086	Sarcolipin	−1.68
Pla2g2a	29692	Phospholipase A2, group IIA (platelets, synovial fluid)	−1.66
Smpd3	94338	Sphingomyelin phosphodiesterase 3, neutral membrane	−1.56
Pltp	296371	Phospholipid transfer protein	−1.45
Slc37a2	500973	Solute carrier family 37 (glycerol-3-phosphate transporter), member 2	−1.38
Chn2	84031	Chimerin (chimaerin) 2	−1.38
Prkcd	170538	Protein kinase C, delta	−1.35
Ldhal6b	369018	Lactate dehydrogenase A-like 6B	−1.35
Scd	83792	Stearoyl-CoA desaturase (delta-9-desaturase)	−1.31

for PLIN5-induced lipid accumulation, we compared these results with overexpression of PLIN2. As described previously [2], PLIN2 overexpression increased IMCL levels concurrent with a gene expression profile favoring lipid storage rather than oxidation. Fig. 4 displays the effects of PLIN5 and PLIN2 electroporation (versus the corresponding empty vector controls) on gene sets involved in fatty acid oxidation and mitochondrial function. Interestingly, PLIN5 has opposite effects on transcription levels of genes involved in FA oxidation compared to PLIN2. Our data indicate that – as opposed to PLIN2 overexpression – PLIN5 overexpression is associated with induction of a transcriptional program favoring FA catabolism and subsequent mitochondrial oxidation. These changes in gene expression were functionally reflected in increased ^{14}C-palmitate oxidation to CO_2 after PLIN5 overexpression which we observed previously (empty vector 0.05 ± 0.008, PLIN5 0.07 ± 0.012 $^{14}CO_2$/total ^{14}C-palmitate oxidation, $P = 0.05$) [8].

3.4. Despite increased IMCL content, PLIN5 overexpression did not impair insulin sensitivity

Skeletal muscle insulin sensitivity was measured under stable clamp conditions (Supplemental Fig. 1). Despite the pronounced effect of PLIN5 overexpression on intramyocellular lipid storage and LD size, ^{3}H-deoxyglucose uptake was similar in empty vector and PLIN5-electroporated muscle (Fig. 5), indicating that PLIN5-induced intramyocellular lipid storage did not impair insulin mediated glucose uptake.

4. Discussion

Elevated IMCL levels have been associated with the development of insulin resistance [24–26], however data from the last decade indicates that the relation between IMCL and insulin sensitivity may be less straightforward than originally proposed [3,4,27]. In recent years, PLINs have been identified as important regulators of skeletal muscle lipid metabolism. Skeletal muscle-specific PLIN2 overexpression improved insulin sensitivity despite increased IMCL levels [2]. Here we show that the augmented IMCL storage as a result of PLIN5 electroporation did not impair insulin-stimulated glucose uptake, consistent with effects of PLIN2 overexpression. Yet, in striking contrast to the effects of PLIN2 overexpression [2], PLIN5 electroporation resulted in a gene expression profile favoring fatty acid catabolism and mitochondrial function. This profile of high PLIN5 levels, augmented IMCL storage, increased oxidative gene expression and fat oxidative capacity without a negative impact on skeletal muscle insulin-mediated glucose uptake mimics observations in master athletes [28].

Both PLIN2 and PLIN5 overexpression resulted in increased LD size, consistent with *in vitro* studies [9,29,30]. When compared to PLIN2-induced LD expansion [2], LDs in PLIN5-overexpressing muscle were approximately 1.3-fold larger in size. While large LDs have previously been suggested to be more detrimental with respect to insulin sensitivity than small LDs [31–33], we here demonstrate that augmenting LD size by overexpressing PLIN5 did not impede insulin-mediated glucose uptake or compromise mitochondrial function measured as fat oxidative capacity within the time frame of our studies.

Table 2
PLIN5 overexpression increased expression of genes involved in mitochondrial function and fatty acid oxidation. Microarray gene expression profiles for PLIN5 overexpression were clustered in Gene Ontology (GO) classes using GSEA (Gene Set Enrichment Analysis). This table shows the GO classes that were enriched in the set of upregulated genes. All upregulated GO classes with a false discovery rate (FDR) q-value <0.05 are shown. NES: normalized enrichment score.

GO	Name	Number of genes in the gene set	NES	FDR q-value
GO:0005759	Mitochondrial matrix	164	4.01	<1.00E-06
GO:0044455	Mitochondrial membrane part	103	3.60	<1.00E-06
GO:0045333	Cellular respiration	60	3.59	<1.00E-06
GO:0005743	Mitochondrial inner membrane	266	3.50	<1.00E-06
GO:0019866	Organelle inner membrane	288	3.30	<1.00E-06
GO:0030964	NADH dehydrogenase complex	31	3.29	<1.00E-06
GO:0045271	Respiratory chain complex I	31	3.28	<1.00E-06
GO:0005747	Mitochondrial respiratory chain complex I	31	3.26	<1.00E-06
GO:0005746	Mitochondrial respiratory chain	46	3.01	<1.00E-06
GO:0022900	Electron transport chain	60	2.98	<1.00E-06
GO:0070469	Respiratory chain	49	2.90	4.52E-05
GO:0006084	Acetyl-CoA metabolic process	45	2.88	1.29E-04
GO:0072329	Monocarboxylic acid catabolic process	54	2.79	2.74E-04
GO:0006091	Generation of precursor metabolites and energy	204	2.76	4.48E-04
GO:0009060	Aerobic respiration	25	2.74	5.01E-04
GO:0015980	Energy derivation by oxidation of organic compounds	117	2.71	6.28E-04
GO:0022904	Respiratory electron transport chain	27	2.67	1.04E-03
GO:0009062	Fatty acid catabolic process	52	2.58	2.97E-03
GO:0046356	Acetyl-CoA catabolic process	22	2.55	3.86E-03
GO:0006119	Oxidative phosphorylation	23	2.48	7.09E-03
GO:0046395	Carboxylic acid catabolic process	120	2.46	7.23E-03
GO:0003954	NADH dehydrogenase activity	19	2.43	8.80E-03
GO:0016054	Organic acid catabolic process	120	2.42	9.12E-03
GO:0048037	Cofactor binding	251	2.42	9.01E-03
GO:0007005	Mitochondrion organization and biogenesis	125	2.40	1.01E-02
GO:0050662	Coenzyme binding	183	2.39	1.08E-02
GO:0006099	Tricarboxylic acid cycle	21	2.39	1.08E-02
GO:0051187	Cofactor catabolic process	30	2.38	1.10E-02
GO:0051186	Cofactor metabolic process	199	2.37	1.20E-02
GO:0006732	Coenzyme metabolic process	158	2.37	1.18E-02
GO:0006637	Acyl-CoA metabolic process	21	2.37	1.16E-02
GO:0009109	Coenzyme catabolic process	25	2.34	1.55E-02
GO:0016655	Oxidoreductase activity, acting on NADH or NADPH, quinone or similar compound as acceptor	21	2.32	1.70E-02
GO:0051262	Protein tetramerization	62	2.32	1.77E-02
GO:0035383	Thioester metabolic process	21	2.32	1.76E-02
GO:0008137	NADH dehydrogenase (ubiquinone) activity	18	2.31	1.76E-02
GO:0042773	ATP synthesis coupled electron transport	18	2.29	2.11E-02
GO:0050136	NADH dehydrogenase (quinone) activity	18	2.29	2.11E-02
GO:0016651	Oxidoreductase activity	53	2.27	2.27E-02
GO:0051087	Chaperone binding	33	2.27	2.23E-02
GO:0019395	Fatty acid oxidation	72	2.24	2.84E-02
GO:0006635	Fatty acid beta-oxidation	39	2.23	3.02E-02
GO:0034440	Lipid oxidation	73	2.23	3.09E-02
GO:0016469	Proton-transporting two-sector ATPase complex	48	2.22	3.16E-02
GO:0005777	Peroxisome	85	2.21	3.39E-02
GO:0042579	Microbody	85	2.19	3.74E-02
GO:0015985	Energy coupled proton transport, down electrochemical gradient	42	2.19	3.96E-02
GO:0015986	ATP synthesis coupled proton transport	42	2.18	4.24E-02
GO:0006818	Hydrogen transport	74	2.17	4.52E-02
GO:0000062	Fatty-acyl-CoA binding	19	2.16	4.49E-02
GO:0031968	Organelle outer membrane	88	2.16	4.54E-02

Table 3
PLIN5 overexpression lowers expression of genes involved in immune processes. Microarray gene expression profiles for PLIN5 overexpression were clustered in Gene Ontology (GO) classes using GSEA (Gene Set Enrichment Analysis). This table shows the GO classes that were enriched in the set of downregulated genes. All downregulated GO classes with a false discovery rate (FDR) q-value <0.05 are shown. NES: normalized enrichment score.

GO	Name	Number of genes in the gene set	NES	FDR q-val
GO:0002252	Immune effector process	249	−2.99	1.60E-03
GO:0004428	Inositol or phosphatidylinositol kinase activity	31	−2.97	1.15E-03
GO:0002768	Immune response-regulating cell surface receptor signaling pathway	66	−2.94	1.40E-03
GO:0002429	Immune response-activating cell surface receptor signaling pathway	63	−2.92	1.41E-03
GO:0002274	Myeloid leukocyte activation	78	−2.83	2.03E-03
GO:0005765	Lysosomal membrane	61	−2.82	1.99E-03
GO:0016050	Vesicle organization	74	−2.80	2.03E-03
GO:0009897	External side of plasma membrane	177	−2.68	5.10E-03
GO:0000323	Lytic vacuole	189	−2.61	7.09E-03
GO:0002443	Leukocyte mediated immunity	146	−2.52	1.18E-02
GO:0005096	GTPase activator activity	138	−2.51	1.25E-02
GO:0050776	Regulation of immune response	297	−2.49	1.34E-02
GO:0046488	Phosphatidylinositol metabolic process	72	−2.49	1.29E-02
GO:0005100	Rho GTPase activator activity	22	−2.47	1.41E-02
GO:0002449	Lymphocyte mediated immunity	118	−2.47	1.36E-02
GO:0046649	Lymphocyte activation	310	−2.47	1.32E-02
GO:0042110	T cell activation	212	−2.46	1.32E-02
GO:0005764	Lysosome	188	−2.44	1.44E-02
GO:0001727	Lipid kinase activity	26	−2.39	1.91E-02
GO:0035586	Purinergic receptor activity	31	−2.39	1.93E-02
GO:0050852	T cell receptor signaling pathway	34	−2.32	2.43E-02
GO:0046854	Phosphatidylinositol phosphorylation	15	−2.32	2.38E-02
GO:0006909	Phagocytosis	64	−2.32	2.36E-02
GO:0050851	Antigen receptor-mediated signaling pathway	54	−2.32	2.35E-02
GO:0006044	N-acetylglucosamine metabolic process	16	−2.28	2.68E-02
GO:0044420	Extracellular matrix part	103	−2.27	2.70E-02
GO:0045058	T cell selection	21	−2.25	2.85E-02
GO:0002460	Adaptive immune response based on somatic recombination of immune receptors built from immunoglobulin superfamily domains	121	−2.24	2.86E-02
GO:0019724	B cell mediated immunity	68	−2.23	3.17E-02
GO:0001614	Purinergic nucleotide receptor activity	27	−2.22	3.13E-02
GO:0046633	Alpha-beta T cell proliferation	20	−2.21	3.23E-02
GO:0006041	Glucosamine metabolic process	16	−2.20	3.28E-02
GO:0016502	Nucleotide receptor activity	27	−2.19	3.48E-02
GO:0010717	Regulation of epithelial to mesenchymal transition	24	−2.17	3.85E-02
GO:0002250	Adaptive immune response	124	−2.16	3.85E-02
GO:0007173	Epidermal growth factor receptor signaling pathway	39	−2.15	4.24E-02
GO:0005581	Collagen	24	−2.14	4.24E-02
GO:0000139	Golgi membrane	265	−2.14	4.19E-02
GO:0050778	Positive regulation of immune response	228	−2.14	4.29E-02
GO:0002062	Chondrocyte differentiation	45	−2.12	4.70E-02
GO:0006040	Amino sugar metabolic process	21	−2.11	4.87E-02
GO:0045061	Thymic T cell selection	16	−2.10	4.99E-02
GO:0007229	Integrin-mediated signaling pathway	46	−2.10	4.95E-02
GO:0045309	Protein phosphorylated amino acid binding	21	−2.10	4.89E-02

One mechanism by which PLINs and an increase in LD size may prevent lipid-induced insulin resistance is by sequestering bioactive lipids. Indeed, PLIN5 overexpression increased intramyocellular TAG storage

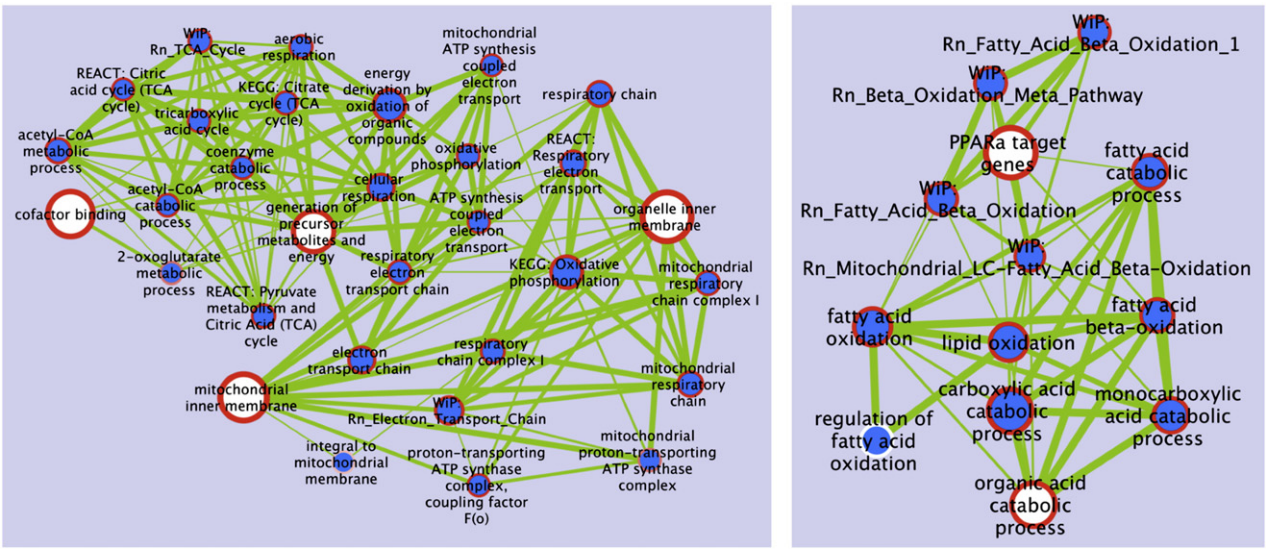

Fig. 4. Gene expression profiles of PLIN5 overexpression were markedly different from those obtained after overexpression of PLIN2. Cytoscape gene set clustering (two selected clusters are shown). The cluster on the left shows gene sets involving mitochondrial function including the TCA cycle and the electron transport chain. The cluster on the right hand side shows gene sets linked to FA oxidative metabolism. Gene expression levels in the PLIN2 and PLIN5 electroporated legs were both compared to the corresponding empty vector legs. The inner circle color corresponds to the effect of PLIN2 overexpression, the circle border represents the effects of PLIN5 overexpression. Blue: downregulation, red: upregulation, white: no change. The lines indicate overlap between gene sets. The gene sets included the GO classes, KEGG pathways, REACT, and WiP gene sets.

without affecting the accumulation of the potentially insulin desensitizing and mitotoxic lipid intermediates DAG and acylcarnitines. These effects parallel observations upon PLIN2 overexpression [2], when IMCL content was also augmented while fatty acid intermediates remained unchanged. Thus, both PLIN2 and PLIN5 overexpression augmented neutral TAG accumulation in a manner that did not impede insulin-mediated glucose uptake.

While the effects of PLIN2 and PLIN5 on IMCL content and insulin sensitivity appear alike, marked differences were observed in gene expression profiles. In striking contrast to the effects of PLIN2 overexpression, which results in lowered expression of genes and proteins involved in oxidative metabolism [2], PLIN5 overexpression resulted in a transcriptomic profile representing improved oxidative capacity. Our unbiased microarray approach raised the opportunity to study gene expression patterns across the whole genome. Gene set enrichment analysis revealed an overrepresentation of upregulated genes in a multiple gene sets involved in FA β-oxidation, the TCA cycle, the electron transport chain and mitochondrion organization. Consistent with our data, ectopic expression of PLIN5 in COS cells increased expression of genes involved in FA oxidation [34]. While short-term (one week) PLIN2 overexpression was beneficial to insulin sensitivity [2], it is anticipated that in the long run, PLIN2 overexpression may result in a mismatch between lipid storage and oxidative capacity. In contrast, PLIN5 overexpression results in increased IMCL storage paralleled with increased oxidative capacity, observations similar to endurance trained athletes who have high PLIN5 and IMCL levels, are insulin sensitive [28] and are protected against lipid-induced insulin resistance [35].

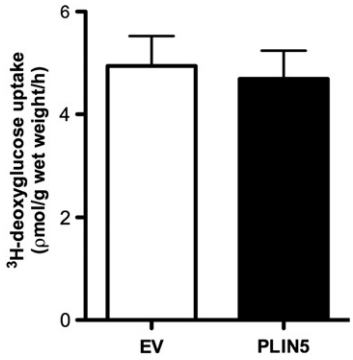

Fig. 5. PLIN5 overexpression-induced intramyocellular lipid accumulation did not affect insulin sensitivity. ^{3}H-labeled deoxyglucose uptake (ρmol/g wet weight/h) in empty vector (EV) and PLIN5-electroporated tibialis anterior muscle (n = 9). Error bars represent SEM.

Since acylcarnitine accumulation has been suggested to reflect an imbalance between β-oxidation and TCA cycle activity [36], the lack of an induction of acylcarnitine accumulation further confirms that PLIN5 overexpression results in neutral IMCL storage matched with downstream catabolic metabolism. Moreover, genes involved in immune-processes associated with insulin resistance were downregulated upon PLIN5 overexpression. Though, whether increased PLIN5 expression is beneficial in the long term, remains to be investigated.

How PLIN5 overexpression promotes oxidative gene expression is currently unknown. It is however of interest to note that the vast majority of the genes induced is under control of the PPAR-PGC1α complex. PPAR-PGC1α mediated gene expression requires fatty acids as ligands. Recent studies in mice lacking the ATGL gene revealed that fatty acids which serve as ligands for PPARs originate from LD lipolysis; lack of ATGL in heart, liver and brown adipose tissue leads to severe reduction of oxidative gene expression [37–39]. It should however be noted that ATGL deficiency in skeletal muscle is not associated with reduced mitochondrial function [40,41]. Yet, we previously showed that ectopic overexpression of PLIN1 in cultured myotubes abolished AGTL mediated lipolysis and downregulated oxidative gene expression [42], which could not be rescued by adding exogenous fatty acids to the medium. This indicates that reduced intramyocellular LD lipolysis modulates gene expression by affecting ligand release from the LD. Along the same lines, one may speculate that overexpression of PLIN5 induces a reversed process. In contrast to overexpressing PLIN1 in muscle, overexpressing PLIN5 may promote liberation of fatty acids from the LD as ligands to promote oxidative gene expression and fat oxidative capacity.

Interestingly, PLIN5 appears to have a dual effect on LD lipolysis. Under basal conditions PLIN5 inhibits lipolysis while under stimulated conditions PLIN5 appears to facilitate lipolysis [43–46]. In the present study PLIN5 overexpression resulted in increased ATGL protein content. Thus, a higher availability of both PLIN5 and ATGL may translate into

increased lipolytic capacity under stimulated conditions and promotes liberation of fatty acids as ligands for the PPAR-PGC1α complex [37]. With that, PLIN5 overexpression might induce a feed-forward loop, since skeletal muscle PGC1α activation is known to affect both oxidative capacity and intracellular lipid storage [47–49]. On the other hand, we also observed that overexpression of PLIN5 resulted in a profound increase in LD size and TAG content which could reflect a state of decreased ATGL-mediated lipolysis and hence blunted availability of fatty acids as ligands. Therefore, it cannot be excluded that PLIN5 may activate PPAR/PGC1 *via* other mechanisms. Based upon subcellular distribution of PLIN5 and its interaction with the mitochondria we previously hypothesized a role for PLIN5 as a chaperone protein shuttling fatty acids towards the mitochondria for oxidation [8]. Similarly, PLIN5 may also be involved in shuttling LD-derived fatty acids towards nuclei to serve as ligands for PPAR/PGC1. In that respect it is of relevance to note that PLIN5 was shown to localize to small, high dense lipid droplets and to be involved in lipid trafficking [29].

Based on previous reports and our current data of improved gene expression of oxidative genes, we propose that PLIN5 is an important player in matching intramyocellular lipid storage capacity with the ability to regulate oxidative gene expression on the one hand and facilitating release of fatty acids from the LD as substrates for mitochondrial oxidation on the other hand.

In summary, PLIN2 and PLIN5 both increase neutral IMCL content without negatively impacting on insulin sensitivity. Interestingly, as opposed to the transcriptomic profile upon PLIN2 overexpression, we here report that overexpression of PLIN5 in skeletal muscle promoted expression of a cluster of genes under control of PPARα and PGC1α involved in fatty acid catabolism and mitochondrial oxidation. This suggests a role of PLIN5, either directly or indirectly, in mediating the skeletal muscle oxidative gene expression.

Supplementary data to this article can be found online at http://dx.doi.org/10.1016/j.bbalip.2013.01.007.

Acknowledgements

Research presented in this article was financially supported by NUTRIM and the graduate school VLAG. A VICI (grant 918.96.618) and a VIDI (grant 917.66.359) for innovative research from the Netherlands Organization for Scientific Research (NWO) support the work of P. Schrauwen and M. Hesselink, respectively. We thank Silvie Timmers, Hazibe Aydeniz and Frits Mattijssen for practical help and technical support.

References

[1] M. Bosma, S. Kersten, M.K.C. Hesselink, P. Schrauwen, Re-evaluating lipotoxic triggers in skeletal muscle: relating intramyocellular lipid metabolism to insulin sensitivity, Prog. Lipid Res. 51 (2012) 36–49.
[2] M. Bosma, M.K.C. Hesselink, L.M. Sparks, S. Timmers, M.J. Ferraz, F. Mattijssen, D. van Beurden, G. Schaart, M.H. de Baets, F.K. Verheyen, S. Kersten, P. Schrauwen, Perilipin 2 improves insulin sensitivity in skeletal muscle despite elevated intramuscular lipid levels, Diabetes 61 (2012) 2679–2690.
[3] L. Liu, X. Shi, C.S. Choi, G.I. Shulman, K. Klaus, K.S. Nair, G.J. Schwartz, Y. Zhang, I.J. Goldberg, Y.H. Yu, Paradoxical coupling of triglyceride synthesis and fatty acid oxidation in skeletal muscle overexpressing DGAT1, Diabetes 58 (2009) 2516–2524.
[4] S. Schenk, J.F. Horowitz, Acute exercise increases triglyceride synthesis in skeletal muscle and prevents fatty acid-induced insulin resistance, J. Clin. Invest. 117 (2007) 1690–1698.
[5] S. Timmers, J. de Vogel-van den Bosch, M.K.C. Hesselink, D. van Beurden, G. Schaart, M.J. Ferraz, M. Losen, P. Martinez-Martinez, M.H. De Baets, J.M.F.G. Aerts, P. Schrauwen, Paradoxical increase in TAG and DAG content parallel the insulin sensitizing effect of unilateral DGAT1 overexpression in rat skeletal muscle, PLoS One 6 (2011) e14503.
[6] M. Beller, K. Thiel, P.J. Thul, H. Jäckle, Lipid droplets: a dynamic organelle moves into focus, FEBS Lett. 584 (2010) 2176–2182.
[7] T.C. Walther, R.V. Farese Jr., The life of lipid droplets, Biochim. Biophys. Acta 1791 (2009) 459–466.
[8] M. Bosma, R. Minnaard, L.M. Sparks, G. Schaart, M. Losen, M.H. De Baets, H. Duimel, S. Kersten, P.E. Bickel, P. Schrauwen, M.K.C. Hesselink, The lipid droplet coat protein perilipin 5 also localizes to muscle mitochondria, Histochem. Cell Biol. 137 (2012) 205–216.
[9] H. Wang, U. Sreenevasan, H. Hu, A. Saladino, B.M. Polster, L.M. Lund, D.W. Gong, W.C. Stanley, C. Sztalryd, Perilipin 5, a lipid droplet associated protein, provides physical and metabolic linkage to mitochondria, J. Lipid Res. 52 (2011) 2159–2168.
[10] C.R. Bruce, C. Brolin, N. Turner, M.E. Cleasby, F.R. van der Leij, G.J. Cooney, E.W. Kraegen, Overexpression of carnitine palmitoyltransferase I in skeletal muscle *in vivo* increases fatty acid oxidation and reduces triacylglycerol esterification, Am. J. Physiol. Endocrinol. Metab. 292 (2007) E1231–E1237.
[11] C.R. Bruce, A.J. Hoy, N. Turner, M.J. Watt, T.L. Allen, K. Carpenter, G.J. Cooney, M.A. Febbraio, E.W. Kraegen, Overexpression of carnitine palmitoyltransferase-1 in skeletal muscle is sufficient to enhance fatty acid oxidation and improve high fat diet-induced insulin resistance, Diabetes 58 (2009) 550–558.
[12] D.E. James, A.B. Jenkins, E.W. Kraegen, Heterogeneity of insulin action in individual muscles *in vivo*: euglycemic clamp studies in rats, Am. J. Physiol. Endocrinol. Metab. 248 (1985) E567–E574.
[13] J.-Y. Kim, T.R. Koves, G.-S. Yu, T. Gulick, R.N. Cortright, G.L. Dohm, D.M. Muoio, Evidence of a malonyl-CoA-insensitive carnitine palmitoyltransferase I activity in red skeletal muscle, Am. J. Physiol. Endocrinol. Metab. 282 (2002) E1014–E1022.
[14] H.R. Scholte, Y. Yu, J.D. Ross, I.I. Oosterkamp, A.M.C. Boonman, H.F.M. Busch, Rapid isolation of muscle and heart mitochondria, the lability of oxidative phosphorylation and attempts to stabilize the process *in vitro* by taurine, carnitine and other compounds, Mol. Cell. Biochem. 174 (1997) 61–66.
[15] B. Ukropcova, M. McNeil, O. Sereda, L. de Jonge, H. Xie, G.A. Bray, S.R. Smith, Dynamic changes in fat oxidation in human primary myocytes mirror metabolic characteristics of the donor, J. Clin. Invest. 115 (2005) 1934–1941.
[16] M.D. Abramoff, P.J. Magalhaes, S.J. Ram, Image processing with Imagej, Biophoton. Int. 11 (2004) 36–42.
[17] R. Koopman, G. Schaart, M. Hesselink, Optimisation of oil red O staining permits combination with immunofluorescence and automated quantification of lipids, Histochem. Cell Biol. 116 (2001) 63–68.
[18] D.M. Schwartz, N.E. Wolins, A simple and rapid method to assay triacylglycerol in cells and tissues, J. Lipid Res. 48 (2007) 2514–2520.
[19] N. Van Vlies, L. Tian, H. Overmars, A.H. Bootsma, W. Kulik, R.J. Wanders, P.A. Wood, F.M. Vaz, Characterization of carnitine and fatty acid metabolism in the long-chain acyl-CoA dehydrogenase-deficient mouse, Biochem. J. 387 (2005) 185–193.
[20] R. Gentleman, V. Carey, D. Bates, B. Bolstad, M. Dettling, S. Dudoit, B. Ellis, L. Gautier, Y. Ge, J. Gentry, K. Hornik, T. Hothorn, W. Huber, S. Iacus, R. Irizarry, F. Leisch, C. Li, M. Maechler, A. Rossini, G. Sawitzki, C. Smith, G. Smyth, L. Tierney, J. Yang, J. Zhang, Bioconductor: open software development for computational biology and bioinformatics, Genome Biol. 5 (2004) R80.
[21] A. Subramanian, P. Tamayo, V.K. Mootha, S. Mukherjee, B.L. Ebert, M.A. Gillette, A. Paulovich, S.L. Pomeroy, T.R. Golub, E.S. Lander, J.P. Mesirov, Gene set enrichment analysis: a knowledge-based approach for interpreting genome-wide expression profiles, Proc. Natl. Acad. Sci. 102 (2005) 15545–15550.
[22] C.T. Lopes, M. Franz, F. Kazi, S.L. Donaldson, Q. Morris, G.D. Bader, Cytoscape Web: an interactive web-based network browser, Bioinformatics 26 (2010) 2347–2348.
[23] T.R. Koves, J.R. Ussher, R.C. Noland, D. Slentz, M. Mosedale, O. Ilkayeva, J. Bain, R. Stevens, J.R.B. Dyck, C.B. Newgard, G.D. Lopaschuk, D.M. Muoio, Mitochondrial overload and incomplete fatty acid oxidation contribute to skeletal muscle insulin resistance, Cell Metab. 7 (2008) 45–56.
[24] C. Aguer, M. Foretz, L. Lantier, S. Hebrard, B. Viollet, J. Mercier, M. Kitzmann, Increased FAT/CD36 cycling and lipid accumulation in myotubes derived from obese type 2 diabetic patients, PLoS One 6 (2011) e28981.
[25] B.H. Goodpaster, R. Theriault, S.C. Watkins, D.E. Kelley, Intramuscular lipid content is increased in obesity and decreased by weight loss, Metabolism 49 (2000) 467–472.
[26] D.A. Pan, S. Lillioja, A.D. Kriketos, M.R. Milner, L.A. Baur, C. Bogardus, A.B. Jenkins, L.H. Storlien, Skeletal muscle triglyceride levels are inversely related to insulin action, Diabetes 46 (1997) 983–988.
[27] J.J. Dubé, F. Amati, M. Stefanovic-Racic, F.G.S. Toledo, S.E. Sauers, B.H. Goodpaster, Exercise-induced alterations in intramyocellular lipids and insulin resistance: the athlete's paradox revisited, Am. J. Physiol. Endocrinol. Metab. 294 (2008) E882–E888.
[28] F. Amati, J.J. Dube, E. Alvarez-Carnero, M.M. Edreira, P. Chomentowski, P.M. Coen, G.E. Switzer, P.E. Bickel, M. Stefanovic-Racic, F.G.S. Toledo, B.H. Goodpaster, Skeletal muscle triglycerides, diacylglycerols, and ceramides in insulin resistance: another paradox in endurance-trained athletes? Diabetes 60 (2011) 2588–2597.
[29] S.R. Bartholomew, E.H. Bell, T. Summerfield, L.C. Newman, E.L. Miller, B. Patterson, Z.P. Niday, W.E. Ackerman Iv, J.T. Tansey, Distinct cellular pools of perilipin 5 point to roles in lipid trafficking, Biochim. Biophys. Acta 1821 (2012) 268–278.
[30] M. Imamura, T. Inoguchi, S. Ikuyama, S. Taniguchi, K. Kobayashi, N. Nakashima, H. Nawata, ADRP stimulates lipid accumulation and lipid droplet formation in murine fibroblasts, Am. J. Physiol. Endocrinol. Metab. 283 (2002) E775–E783.
[31] M. Fraenkel, R. Weiss, I. Leizerman, D. Anaby, E. Golomb, G. Leibowitz, N. Kaiser, Scanning electron microscopic analysis of intramyocellular lipid droplets in an animal model of type 2 diabetes, Obesity 16 (2008) 695–699.
[32] J. He, B.H. Goodpaster, D.E. Kelley, Effects of weight loss and physical activity on muscle lipid content and droplet size, Obesity 12 (2004) 761–769.
[33] J.C. Molero, S. Lee, I. Leizerman, A. Chajut, A. Cooper, K. Walder, Effects of rosiglitazone on intramyocellular lipid accumulation in Psammomys obesus, Biochim. Biophys. Acta 1802 (2010) 235–239.
[34] N.E. Wolins, B.K. Quaynor, J.R. Skinner, A. Tzekov, M.A. Croce, M.C. Gropler, V. Varma, A. Yao-Borengasser, N. Rasouli, P.A. Kern, B.N. Finck, P.E. Bickel, OXPAT/PAT-1 is a PPAR-induced lipid droplet protein that promotes fatty acid utilization, Diabetes 55 (2006) 3418–3428.
[35] E. Phielix, R. Meex, D.M. Ouwens, L. Sparks, J. Hoeks, G. Schaart, E. Moonen-Kornips, M.K.C. Hesselink, P. Schrauwen, High oxidative capacity due to chronic exercise training attenuates lipid-induced insulin resistance, Diabetes 62 (2012) 2472–2478.

[36] D.M. Muoio, Intramuscular triacylglycerol and insulin resistance: guilty as charged or wrongly accused? Biochim. Biophys. Acta 1801 (2009) 281–288.
[37] G. Haemmerle, T. Moustafa, G. Woelkart, S. Buttner, A. Schmidt, T. van de Weijer, M. Hesselink, D. Jaeger, P.C. Kienesberger, K. Zierler, R. Schreiber, T. Eichmann, D. Kolb, P. Kotzbeck, M. Schweiger, M. Kumari, S. Eder, G. Schoiswohl, N. Wongsiriroj, N.M. Pollak, F.P.W. Radner, K. Preiss-Landl, T. Kolbe, T. Rulicke, B. Pieske, M. Trauner, A. Lass, R. Zimmermann, G. Hoefler, S. Cinti, E.E. Kershaw, P. Schrauwen, F. Madeo, B. Mayer, R. Zechner, ATGL-mediated fat catabolism regulates cardiac mitochondrial function *via* PPAR-α and PGC-1, Nat. Med. 17 (2011) 1076–1085.
[38] E.P. Mottillo, A.E. Bloch, T. Leff, J.G. Granneman, Lipolytic products activate peroxisome proliferator-activated receptor (PPAR) α and δ in brown adipocytes to match fatty oxidation with supply, J. Biol. Chem. 287 (2012) 25038–25048.
[39] K.T. Ong, M.T. Mashek, S.Y. Bu, A.S. Greenberg, D.G. Mashek, Adipose triglyceride lipase is a major hepatic lipase that regulates triacylglycerol turnover and fatty acid signaling and partitioning, Hepatology 53 (2011) 116–126.
[40] A.J. Hoy, C.R. Bruce, S.M. Turpin, A.J. Morris, M.A. Febbraio, M.J. Watt, Adipose triglyceride lipase-null mice are resistant to high-fat diet-induced insulin resistance despite reduced energy expenditure and ectopic lipid accumulation, Endocrinology 152 (2011) 48–58.
[41] P.M. Nunes, T. van de Weijer, A. Veltien, H. Arnts, M.K.C. Hesselink, J.F.C. Glatz, P. Schrauwen, C.J. Tack, A. Heerschap, Increased intramyocellular lipids but unaltered *in vivo* mitochondrial oxidative phosphorylation in skeletal muscle of adipose triglyceride lipase-deficient mice, Am. J. Physiol. Endocrinol. Metab. 303 (2012) E71–E81.
[42] T.R. Koves, L.M. Sparks, J.P. Kovalik, M. Mosedale, R. Arumugam, K.L. Debalsi, K. Everingham, L. Thorne, E. Phielix, R.C. Meex, C.L. Kien, M.K. Hesselink, P. Schrauwen, D.M. Muoio, PPARγ coactivator-1α contributes to exercise-induced regulation of intramuscular lipid droplet programming in mice and humans, J. Lipid Res. 54 (2013) 522–534.
[43] J.G. Granneman, H.P.H. Moore, E.P. Mottillo, Z. Zhu, L. Zhou, Interactions of perilipin-5 (PLIN5) with adipose trigylceride lipase (ATGL), J. Biol. Chem. 286 (2011) 5126–5135.
[44] J.G. Granneman, H.P. Moore, E.P. Mottillo, Z. Zhu, Functional interactions between MLDP (LSDP5) and ABHD5 in the control of intracellular lipid accumulation, J. Biol. Chem. 284 (2009) 3049–3057.
[45] K. Kuramoto, T. Okamura, T. Yamaguchi, T.Y. Nakamura, S. Wakabayashi, H. Morinaga, M. Nomura, T. Yanase, K. Otsu, N. Usuda, S. Matsumura, K. Inoue, T. Fushiki, Y. Kojima, T. Hashimoto, F. Sakai, F. Hirose, T. Osumi, Perilipin 5, a lipid droplet-binding protein, protects the heart from oxidative burden by sequestering fatty acid from excessive oxidation, J. Biol. Chem. 287 (2012) 23852–23863.
[46] H. Wang, M. Bell, U. Sreenevasan, H. Hu, J. Liu, K. Dalen, C. Londos, T. Yamaguchi, M.A. Rizzo, R. Coleman, D. Gong, D. Brasaemle, C. Sztalryd, Unique regulation of adipose triglyceride lipase (ATGL) by perilipin 5, a lipid droplet-associated protein, J. Biol. Chem. 286 (2011) 15707–15715.
[47] D.O. Espinoza, L.G. Boros, S. Crunkhorn, H. Gami, M.-E. Patti, Dual modulation of both lipid oxidation and synthesis by peroxisome proliferator-activated receptor-γ coactivator-1α and -1β in cultured myotubes, FASEB J. 24 (2010) 1003–1014.
[48] E. Mormeneo, C. Jimenez-Mallebrera, X. Palomer, V. De Nigris, M. Vázquez-Carrera, A. Orozco, A. Nascimento, J. Colomer, C. Lerín, A.M. Gómez-Foix, PGC-1α induces mitochondrial and myokine transcriptional programs and lipid droplet and glycogen accumulation in cultured human skeletal muscle cells, PLoS One 7 (2012) e29985.
[49] S. Summermatter, O. Baum, G. Santos, H. Hoppeler, C. Handschin, Peroxisome proliferator-activated receptor γ coactivator 1α (PGC-1α) promotes skeletal muscle lipid refueling *in vivo* by activating *de novo* lipogenesis and the pentose phosphate pathway, J. Biol. Chem. 285 (2010) 32793–32800.